ISSN 1027-4510, Journal of Surface Investigation: X-ray, Synchrotron and Neutron Techniques, 2023, Vol. 17, Suppl. 1, pp. S233–S238. © Pleiades Publishing, Ltd., 2023.

Optimization of the Design and Parameters of a Double-Mirror Monochromator for the Fourth-Generation SKIF Synchrotron Light Source

E. I. Glushkov[a, *], I. V. Malyshev[a], E. V. Petrakov[a], N. I. Chkhalo[a], Yu. V. Khomyakov[b], Ya. V. Rakshun[b], V. A. Chernov[b], and I. P. Dolbnya[c]

[a] *Institute for Physics of Microstructures, Russian Academy of Sciences, Nizhny Novgorod, 603950 Russia*

[b] *Budker Institute of Nuclear Physics, Siberian Branch, Russian Academy of Sciences, Novosibirsk, 630090 Russia*

[c] *Diamond Light Source, Harwell Science and Innovation Campus, Didcot, Oxfordshire, OX11 0DE United Kingdom*

**e-mail: eglushkov@ipmras.ru*

Received January 25, 2023; revised March 30, 2023; accepted March 30, 2023

Abstract—Synchrotron radiation incident on a block of multilayer X-ray mirrors of a two-mirror monochromator heats a silicon substrate, which leads to thermal deformation and an increase in the angular error of the surface shape. The work examines the heating of a block of multilayer X-ray mirrors by a synchrotron beam with a power of up to 200 W with an energy in the range of 8–36 keV at grazing angles of incidence in the range of 0.5°–1.3°. Using SolidWorks software, the silicon-substrate parameters for mirrors with grooves on the end surface are calculated at which the root-mean-square deviation of the angular error of the substrate's surface shape is about 1 μrad for a grazing angle of 1.3°, and for smaller angles it is less than 1 μrad. Heat is removed from the substrate surface by water using copper radiators. Reducing the beam aperture at the monochromator output makes it possible to obtain rays reflected from the surface of mirrors, which has a standard deviation of the surface shape of an order of 0.5 μrad, while maintaining 88% of the initial beam power at a grazing angle of 1.3°. The use of a piezoelectric actuator to correct the substrate's surface shape makes it possible to reduce the root-mean-square shape error to 0.1 μrad and 0.05 μrad at grazing angles of 0.9° and 0.5°, respectively.

Keywords: synchrotron radiation, multilayer X-ray mirrors, thermal analysis, angular errors, silicon substrate

DOI: 10.1134/S1027451023070133

INTRODUCTION

At the fourth-generation synchrotron radiation (SR) source SKIF, which is being developed at the Siberian Branch, Russian Academy of Sciences, it is planned to use multilayer X-ray mirrors (MXM) for various applications. In particular, at the experimental Station 1-1 Microfocus [1, 2] (Fig. 1), for SR monochromatization it is planned to use a double-mirror monochromator (DMM) with a tunable X-ray wavelength [3, 4]. Station 1-1 Microfocus will take advantage of generation 4+ synchrotrons and will allow high-energy coherent diffraction tomography with a resolution of less than 5 nm, conduct static studies of the states of substances at pressures of up to several million atmospheres and at temperatures of up to thousands of degrees, and solve a number of other problems.

An important factor limiting the working range of grazing angles is the high SR power flux density, especially on the first block of the DMM mirrors [5–7], leading to its heating and deformation. To reduce the root-mean-square deviation (RMS) of the angular shape error of mirrors (which is numerically equal to the derivative of the deformation profile along the

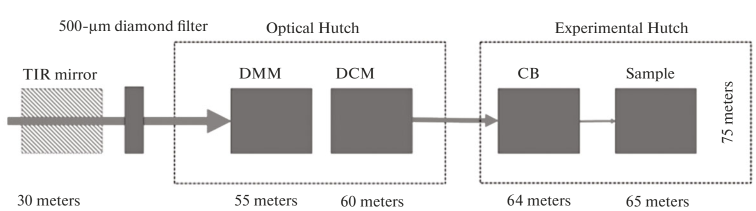

Fig. 1. Optical diagram of experimental Station 1-1 Microfocus [1, 2].

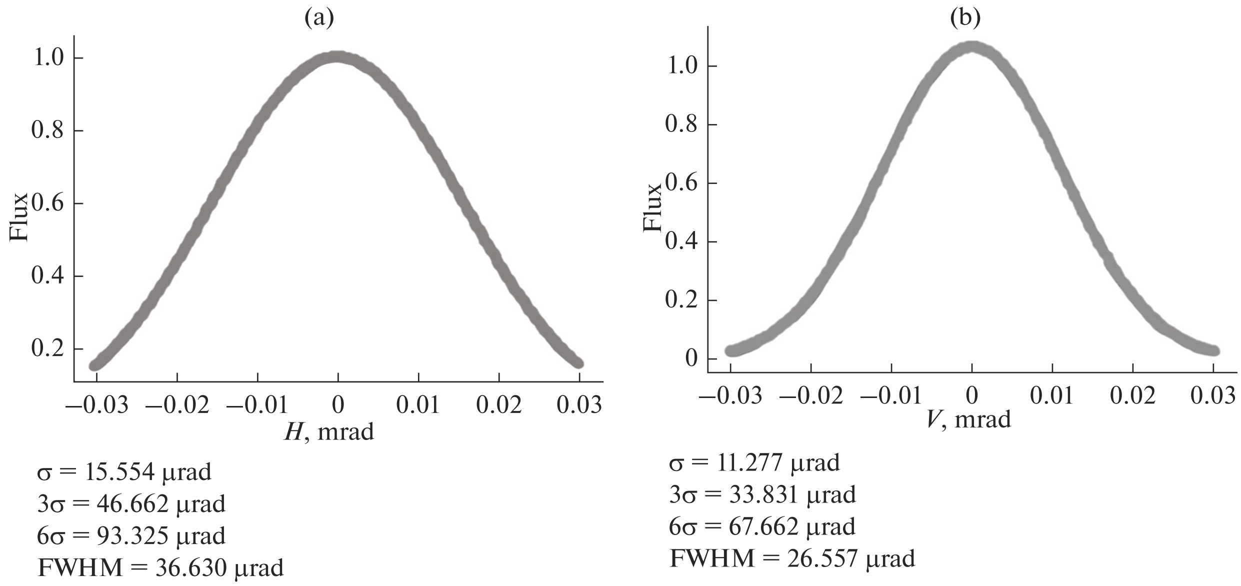

Fig. 2. Photon fluxes in the horizontal (a) and vertical (b) directions. Curves were calculated using the SPECTRA program [16–20].

mirror) which occurs during the manufacture of their silicon substrates, the technology [8] is used, which consists in the machining of grooves of certain sizes on the end surface of the substrate, which leads to a decrease in the angular error of the shape of the mirrors.

In a number of experiments at Station 1-1 Microfocus, it is necessary to use a double-crystal monochromator at the output of a double-mirror monochromator (DMM). This imposes restrictions on the root-mean-square beam divergence at the DMM output, which should not exceed 1 μrad.

This paper presents the results of optimizing the DMM parameters in order to minimize the angular error in the shape of the mirrors that occurs when the substrate on which the MXMs are located is deformed due to heating by a SR beam with a given photon flux and emission spectrum.

MODELING THE GEOMETRICAL PARAMETERS OF MIRROR SUBSTRATES OF A DOUBLE-MIRROR MONOCHROMATOR

Modeling of the External Dimensions and Grooves of the First DMM Block

To reflect the maximum power of incident SR, deposition of the largest possible mirrors is required. The maximum MXM size along the incident SR beam is limited by the silicon-substrate manufacturing technology developed at the Institute for Physics of Microstructures, Russian Academy of Sciences, with a value of 250 mm. Considering the longitudinal size of exposed area on the substrate (Fig. 2a), the MXM with a length of 250 mm will receive from 78.5 to 100% of the power for grazing angles from 0.5° to 1.3°, respectively.

Taking into account the transverse flow distribution (Fig. 2b), a 4-mm-wide MXM makes it possible to capture 99.9% of power.

Thus, the 250 × 4-mm MXM captures from 78.4 to 99.9% of the incident power for grazing angles of 0.5°–1.3°.

Heat can be removed from the substrate using liquid cooling via the substrate ends [9]. Let us set the convective-heat-transfer coefficient equal to 3 $kWm^{-2} K^{-1}$, which is used in similar calculations and is confirmed by the coolant temperature measurements at the monochromator inlet and outlet in similar systems [10–12]. The coolant (water) temperature is set slightly above room temperature (25°C).

It is planned to use 3 MXMs, separated by a distance of 1.5 mm and tuned to various subbands of photon energies in the range of 8–36 keV [2].

Grooves are applied from the lower boundary of the radiators (Fig. 3) and should not pass under the MXMs, because the surface above the grooves may be deformed during manufacturing, which will lead to additional angular error not associated with DMM heating. The depth of grooves was chosen such that the standard deviation of the angular error at a grazing angle of 1.3° was about 1 μrad. With this approach, the angular error for smaller grazing angles turns out to be less than 1 μrad.

The block of mirrors of the DMM and the flow distribution have a common symmetry plane, perpendicular to the block surface, so numerical modeling was carried out only for half of the block of mirrors. Substrate deformations were calculated in the SolidWorks program for isotropic silicon. The SR power-flux density distribution incident on the surface of the block of

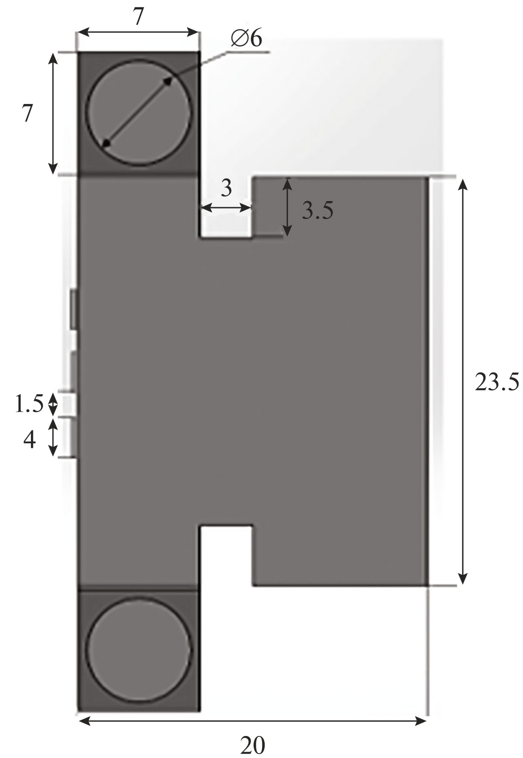

Fig. 3. Scheme of the DMM first mirror. A silicon wafer with grooves and three MXMs on it. The first mirror is located at the substrate center and neighboring mirrors are located on the sides at a distance of 1.5 mm. The mirror is cooled in the upper and lower parts by water flowing through copper radiators. Between the radiators and the substrate there is an indium gasket 0.2 mm thick. In the diagram, all dimensions are given in mm.

mirrors was obtained using XRayTracer [13, 14], taking into account the reflection curves of mirrors that are optimal for the selected range of radiation energies [2], which were calculated using Multifitting [15].

Comparing the surface deformation profiles at different grazing angles, it can be seen (Fig. 4) that at a grazing angle of 1.3°, the deformation profile has a derivative close to zero in the range from 0 to 60 mm, which sharply increases in the range from 60 to 113 mm. This behavior of the deformation curve is due to the fact that the parameters of the grooves were chosen optimal for a grazing angle of 1.3°, for which the standard deviation of the angular error is 1.08 μrad. At grazing angles of 0.9° and 0.5°, the deformation profile has a parabolic shape with a "hook" near the edge of the mirror (inflection on the right), and the standard deviation is 0.34 and 0.21 μrad, respectively.

METHODS FOR CORRECTING THE DIVERGENCE OF A SYNCHROTRON-RADIATION BEAM AT THE OUTPUT OF A DOUBLE-MIRROR MONOCHROMATOR

Reducing the Beam Size

At a grazing angle of 1.3°, the main contribution to the beam divergence comes from deformations near the mirror edges. If we reduce the beam aperture at the DMM output (Fig. 4a, Table 1), then we can eliminate the rays reflected from the mirror edges and retain the rays reflected from the mirror area with a standard deviation of the angular shape error of less than 1 μrad at a relatively small, about 20%, loss of radiation power reflected from the first DMM mirror.

At grazing angles of 0.9° and 0.5°, this method does not significantly reduce the divergence of beams at the DMM output due to the linearity of the derivative of the parabolic deformation profile. However, they are at a fairly low level, less than the typical width of the reflection curve of a crystal monochromator.

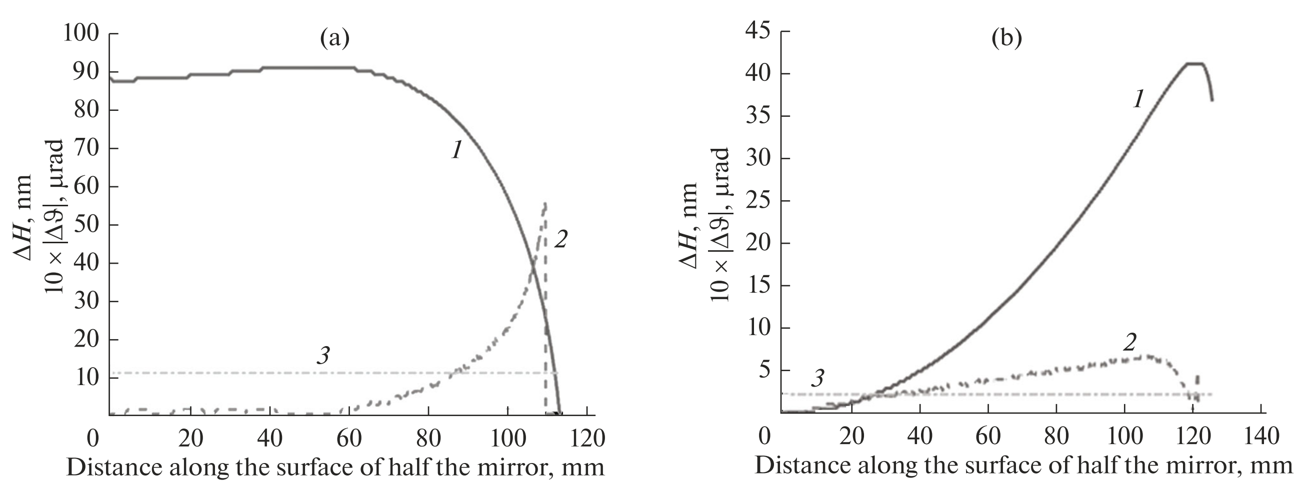

Fig. 4. Surface-deformation profile (*1*), angular error (*2*), and standard deviation of the angular error (*3*) at grazing angles of 1.3° (a) and 0.5° (b).

Table 1. In the cells corresponding to one grazing angle, the first line shows the standard-deviation values of the angular error (μrad); in the second, the power-flux percentage of incident SR passing through the aperture at the DMM output

Grazing angle	Aperture, mm				
	250	200	180	160	140
1.3°	1.08 100%	0.52 88%	0.32 80%	0.19 70%	0.12 60%
0.9°	0.34 100%	0.32 80%	0.29 72%	0.26 64%	
0.5°	0.21 100%	0.19 80%	0.18 72%	0.17 64%	

Using a Piezoelectric Actuator

The deformation profile of a silicon substrate at grazing angles of 0.9° and 0.5° has the shape of a parabola (Fig. 4b) with "hooks" near the mirror edges. By reducing the beam aperture after the DMM, it is possible to eliminate the rays reflected from the DMM edges, which makes it possible to consider in further modeling only the area with a parabolic form of surface deformation.

Let us consider the impact of force $F(x_0)$ on the substrate back side (Fig. 5). Deformation of the beam surface $f_b(x, z)$ under the influence of SR incident at an angle of 0.9° to the beam surface is determined by the results of the previous simulation. Let us apply a force such that the deformation at point x_0 becomes zero (Fig. 5a).

According to mathematical-modeling results, the standard deviation of angular errors of the shape of the surface of mirrors, from which SR is reflected decreases from 0.34 to 0.1 μrad and from 0.21 to 0.05 μrad at grazing angles of 0.9° and 0.5°, respectively.

Thus, a multilayer mirror design and methods have been found to minimize thermally induced deviations of the reflected wave fronts to the level required for the operation of a crystal monochromator.

SECOND DMM BLOCK HEATING

Let us consider heating of the second DMM block by an X-ray beam reflected from the Mo/B4C MXM [2], located in the DMM first block, which serves to reflect photons in the soft energy range of 8–14 keV. In front of the first DMM block there can be a 500-μm diamond filter that transmits 53.56% of the incident radiation power and eliminates two low-energy harmonics of radiation received at the undulator output (Fig. 6). The first harmonic is incident under total external reflection from Mo/B4C in the angle range 0.5°–1.3°. Resonant harmonics of 8100, 10266, and 12210 eV, incident in the soft range, are reflected at Bragg angles of 1.216°, 0.96°, and 0.806°, respectively.

When SR is incident on DMM mirrors at angles of 1.216°, 0.96°, and 0.806°, the absorption of the second block without using a filter is 3.75, 4.26, and 3.76% of the total incident power, respectively; and with a 500-μm diamond filter, it is 1.59, 1.34, and 1.72%, respectively.

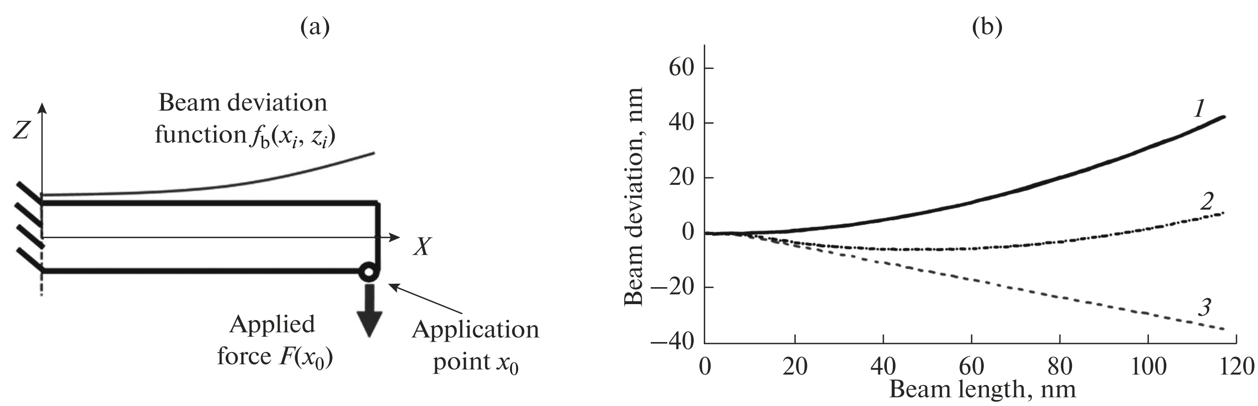

Fig. 5. (a) Diagram of force application to a rigidly clamped beam. (b) Numerical-simulation results of the deviation of a beam rigidly clamped by a piezoelectric actuator. Deformation of a beam under the action of SR incident at a grazing angle of 0.9° (*1*); beam deformation under the influence of SR and the piezoelectric actuator (*2*); deformation of the beam under the action of the piezoelectric actuator (*3*).

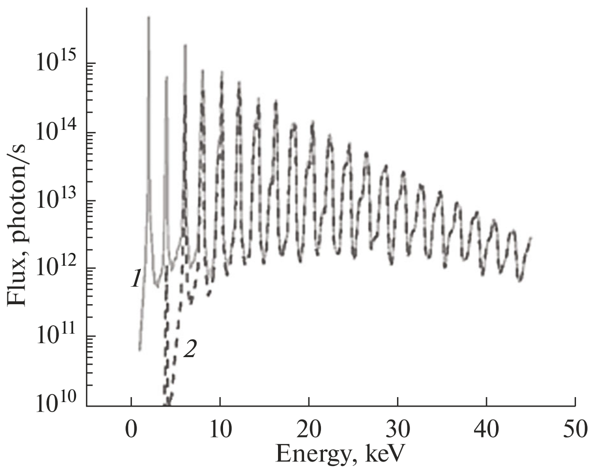

Fig. 6. Dependence of the photon flux on energy without using a filter (*1*) and with a 500-μm diamond filter (*2*). Curves were calculated using the SPECTRA program [13–17].

Let us consider the resulting angular error in the shape of the substrate DMM second mirror in the case when the beam is incident on the DMM at an angle of 1.3°; the beam power reflected from the first mirror is 95% of the initial power; the design of the second block of mirrors is simplified and differs from the first one in the absence of grooves. If the second block of DMM mirrors does not have grooves, then with a decrease in the beam aperture at the DMM output, the standard deviation of the total angular error will lie in the range of 0.19–1.58 μrad with a transmission of 60–100% of the power of the reflected rays. If the second block of DMM mirrors has grooves, then the standard deviation will lie in the range of 0.12–1.13 μrad with a transmission of 60–100% of power of the reflected rays.

CONCLUSIONS

In this work, the parameters of heating a two-mirror monochromator based on multilayer X-ray mirrors are calculated. The optimal geometric dimensions of grooves on the first block of the DMM mirrors were found, which makes it possible to obtain a monochromatic-beam divergence of less than 1 μrad.

Reducing the beam aperture at the DMM output at grazing angles of 1.3° makes it possible to transmit 70–88% of the SR power with a beam divergence caused by thermally induced deformation of the substrate of 0.2–0.5 μrad.

The use of piezoceramics at grazing angles of 0.9° and 0.5° makes it possible to transmit 94% of the radiation power and reduce the beam divergence from 0.35 to 0.1 μrad and from 0.2 to 0.05 μrad, respectively.

Taking into account the heating of the second block of DMM mirrors leads to an increase in the beam divergence to 0.63 μrad without the use of grooves on the second mirror and to 0.54 μrad with their use, when transmitting 88% of power of the reflected rays. That is, the use of grooves on the second mirror does not lead to a significant reduction in the beam divergence, since only 5% of the SR power arrives at the second mirror and is therefore effectively removed by liquid cooling.

FUNDING

This work was supported by the Ministry of Science and Higher Education of the Russian Federation, agreement no. 075-15-2021-1362.

CONFLICT OF INTEREST

The authors of this work declare that they have no conflicts of interest.

REFERENCES

1. S. V. Rashchenko, M. A. Skamarokha, G. N. Baranov, Y. V. Zubavichus, and Ya. V. Rakshun, AIP Conf. Proc. **2299**, 060001 (2020). https://doi.org/10.1063/5.0030346
2. N. I. Chkhalo, S. A. Garakhin, I. V. Malyshev, V. N. Polkovnikov, M. N. Toropov, B. A. Ulasevich, Ya. V. Rakshun, V. A. Chernov, I. P. Dolbnya, and S. V. Rashchenko Nanofiz., Nanoelektron. **1**, 626 (2022). https://doi.org/10.21883/JTF.2022.08.52794.100-22
3. C. Morawe, D. Carau, and J. C. Peffen, SPIE Proc. **10386**, 1038603 (2017). https://doi.org/10.1117/12.2273609
4. R. Dietsch, A. Rack, T. Weitkamp, M. Riotte, T. Rack, T. Holz, M. Kramer, D. Weissbach, C. Morawe, F. Siewert, M. Meduna, P. Cloetens, and E. Ziegler, AIP Conf. Proc. **1365**, 77 (2011). https://doi.org/10.1063/1.3625308
5. A. M. Khounsary, SPIE Proc. **3773**, 78 (1999). https://doi.org/10.1117/12.370114
6. M. Mattenet, D. Abernathy, F. Zontone, C. Detlefs, G. Grubel, M. Facchini, and P. Jacquot, Nucl. Instrum. Methods Phys. Res., Sect. A **467**, 305 (2001). https://doi.org/10.1016/S0168-9002(01)00309-6
7. L. Zhang, R. Barret, K. Friederich, P. Glatzel, T. Mairs, P. Marion, G. Monaco, C. Morawe, and T. Weng, J. Phys.: Conf. Ser. **425**, 052029 (2013). https://doi.org/10.1088/1742-6596/425/5/052029
8. K. J. S. Sawhney, I. P. Dolbnya, S. M. Scott, M. K. Tiwari, G. M. Preece, S. G. Alcock, and A. W. Malandain, SPIE Proc. **8139**, 79 (2011). https://doi.org/10.1117/12.894920
9. Y. Li, A. M. Khounsary, and S. Nair, SPIE Proc. **5533**, 157 (2004). https://doi.org/10.1117/12.561435
10. P. Brumund, J. Reyes-Herrera, C. Morawe, T. Dufrane, H. Isern, T. Brochard, M. Del Rio Sanchez, and C. Detlefs, J. Synchrotron Radiat. **28**, 1423 (2021). https://doi.org/10.1107/S160057752100758X

11. L. Zhang, W. K. Lee, M. Wulff, and L. Eybert, J. Synchrotron Radiat. **10**, 313 (2003). https://doi.org/10.1107/S0909049503012135
12. A. I. Chumakov, I. Sergeev, J. P. Celse, R. Ruffer, M. Lesourd, and L. Zhang, J. Synchrotron Radiat. **21**, 315 (2014). https://doi.org/10.1107/S1600577513033158
13. T. S. Plivelic, A. E. Terry, R. Appio, K. Theodor, and K. Klementiev, AIP Conf. Proc. **2054**, 030013 (2019). https://doi.org/10.1063/1.5084576
14. K. Klementiev and R. Chernikov, XRayTarcer program (2014). https://doi.org/10.5281/zenodo.1252469
15. M. Svechnikov, J. Appl. Crystallogr. **53**, 244 (2020). https://doi.org/10.1107/S160057671901584X
16. T. Tanaka, J. Synchrotron Radiat. **28**, 1267 (2021). https://doi.org/10.1107/S1600577521004100
17. T. Tanaka and H. Kitamura, J. Synchrotron Radiat. **8**, 1221 (2001). https://doi.org/10.1107/S090904950101425X
18. T. Tanaka, Phys. Rev. Spec. Top.—Accel. Beams **17**, 060702 (2014). https://doi.org/10.1103/PhysRevSTAB.17.060702
19. T. Tanaka, Opt. Lett. **42**, 1576 (2017). https://doi.org/10.1364/OL.42.001576
20. T. Tanaka, Phys. Rev. Accel. Beams **21**, 110704 (2018). https://doi.org/10.1103/PhysRevAccel-Beams.21.110704

Translated by V. Selikhanovich